Research Article

A novel chaos-based modulation scheme: adaptive threshold level chaotic on–off keying for increased BER performance

Kenan ALTUN[1,*] , **Enis GÜNAY**[2]

[1]Department of Electronics and Automation, Sivas Vocational College, Sivas Cumhuriyet University, Sivas, Turkey
[2]Department of Electrical and Electronics Engineering, Faculty of Engineering, Erciyes University, Kayseri, Turkey

Abstract: A novel modulation scheme called adaptive threshold level-chaotic on–off keying (ATL-COOK) is proposed. This scheme is applied to direct chaotic communication (DCC) systems where the chaotic signals are used as carrier signals. The objective of the proposed adaptive method is to increase the low BER versus SNR performance caused by the constant threshold voltage level. In the proposed method, the communication signal received by the receiver circuits was defined as a Dirac delta function and a comparison signal was obtained from this signal. Then the BER versus SNR performance was analyzed and compared with that of various chaotic generator structures by using an instantaneous adaptive signal instead of a constant threshold voltage in the receiver circuit decision block. Both the simulation results and the experiments show the efficiency of the proposed method.

Key words: Direct chaotic communication system, field programmable analogue arrays, bit error rate

1. Introduction

In the last century, chaos theory was applied in many different fields of science. It is noteworthy due to its approaches in introducing system behavior and problem solving. Chaos theory studies, specifically in medicine, engineering, and mathematics, contribute to the introduction of novel techniques, models, and research areas [1]. The chaotic signals generated by chaos-based generators stand out with their unpredictability despite their deterministic structure and their high sensitivity to the initial values of system behavior.

Many of the chaotic systems are noise-like and they have a wideband spectrum. Wideband chaotic signals bear the information signals in communication systems. Therefore, the use of chaotic signals in communication systems has increased [2]. Direct chaotic communication (DCC) systems, where the chaotic signal is directly used as an information carrier signal, can be categorized as coherent and noncoherent modulation techniques. The most important problem in chaos-based communication systems is the necessity of recovering the carrier signals in the receiver circuit. Furthermore, the high sensitivity to the initial conditions complicates the recovery and synchronization of chaos signals in the receiver circuits. Therefore, digital noncoherent communication systems that do not require continuous synchronization have begun to gain importance [3, 4]. It is valid for systems where both the chaotic and the periodic signals are used as carriers [5].

Noncoherent, instantly synchronized DCC systems that are used in digital information transmission utilize techniques such as chaos shift keying (CSK) [6], chaotic on–off keying (COOK) [7], differential chaos shift keying (DCSK) [8, 9], and quadrature chaos shift keying (QCSK) [10]. Digital communication systems

---

*Correspondence: kaltun@cumhuriyet.edu.tr

that are implemented using chaotic generators have become an alternative for conventional communication systems due to their simple chaotic circuit structure, wideband carrier signals, and noise-like chaotic signals [11]. The information signal is obtained through a decision block in the receiver circuits of these communication systems. The decision is made with constant threshold voltage level at the comparator input of the decision blocks. It complicates the recovery of the transmitted information signals at the receiver circuits. Therefore, using a constant threshold voltage level, although the noise level at the transmission medium is variable, makes the transmission of the information signal difficult and increases the bit error rate.

The proposed study aims to decrease the bit error rate by determining an adaptive threshold voltage level in the decision blocks of the DCC systems' receiver circuits. In the proposed chaotic communication system, different chaotic generators were designed with a novel communication model that has an adaptive threshold voltage level and simulation results were obtained. In Section 2, the novel model ATL-COOK is introduced. In Section 3 and Section 4, the simulation results and the experimental results that were obtained using different chaotic signals are presented respectively. The final section includes conclusions and discussions.

2. Proposed method ATL-COOK

In DCC systems, the information is transmitted by using the chaotic signals as carriers similar to conventional communication systems. The carrier signals in the transmitter circuits must be recovered in the receiver circuits to transmit the information signal. In DCC systems, the carrier signal is recovered in the receiver circuit through instantaneous or continuous synchronization. The implementation of chaotic communication systems that require continuous synchronization is difficult due to many reasons such as the sensitivity of the initial conditions of the chaotic generators [12, 13]. Therefore, it is much easier to use instantly synchronized DCC systems in chaotic communication systems. In this section, the COOK modulation method, which is an instance of a DCC system, will be explained briefly before the introduction of the proposed ATL-COOK method.

The block schemes of the transmitter and receiver structures for COOK communication systems are shown in Figure 1. The transmitted signal s(t) is generated by switching the chaos signal with the information signal. The generated signal is expressed by Equation 1.
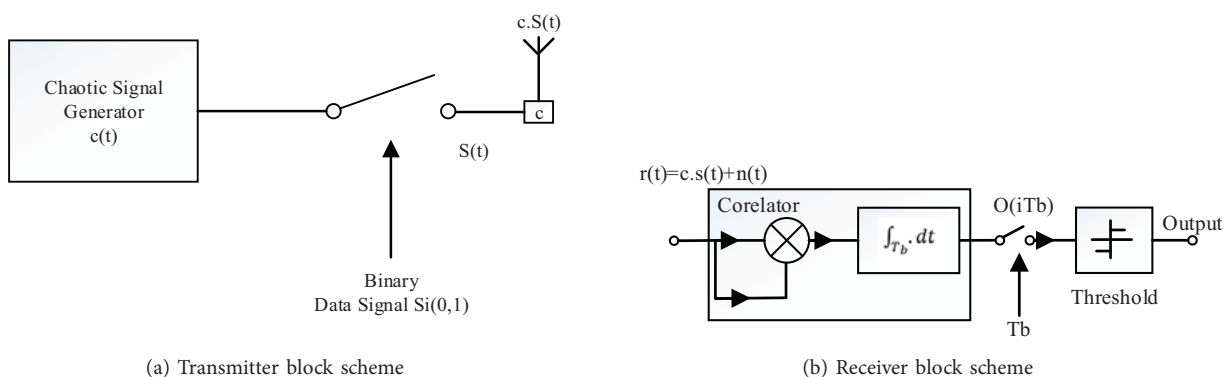

(a) Transmitter block scheme   (b) Receiver block scheme

Figure 1. COOK block scheme.

$$s(t) = \begin{cases} c(t), & \text{when symbol "1" is transmitted} \\ 0, & \text{when symbol "0" is transmitted} \end{cases} \tag{1}$$

The noise signal is added to the signal s(t) that comes from the digital modulator circuit, and then it is transmitted to the receiver circuit along the transmission line. The signal r(t) at the receiver input is correlated

with itself, transferred to the integrator, and sent to the threshold detector. The signal energy at the output of the correlator in noisy situations is expressed by Equation 2. Moreover, the signal energy at the output of the correlator in noiseless condition is expressed by Equation 3 [14]. Since the second and third integrals of Equation 2 in the noiseless condition will be zero, the expression becomes Equation 3.

$$o(iT_b) = \int_{(i-1)T_b}^{iT_b} r^2(t)dt = \int_{(i-1)T_b}^{iT_b} [c.s(t) + n(t)]^2 \, dt$$

$$= \int_{(i-1)T_b}^{iT_b} c^2.s^2(t)dt + 2 \int_{(i-1)T_b}^{iT_b} c.s(t)n(t)dt + \int_{(i-1)T_b}^{iT_b} n^2(t)dt \tag{2}$$

$$o(iT_b) = \begin{cases} \int_{(i-1)T_b}^{iT_b} c^2(t)dt, & \text{"1" is transmitted} \\ 0, & \text{"0" is transmitted} \end{cases} \tag{3}$$

Every symbol in the signal that is integrated in the threshold detector circuit is sampled with a detector that has a zero threshold voltage level at the switching period T_b. Then the output becomes +1 if the signal is positive and 0 otherwise.

The proposed ATL-COOK method has the same transmitter circuit with COOK. However, the constant threshold voltage was replaced with an adaptive threshold voltage at the information signal decision block of the receiver circuit. DCC communication systems with noncoherent modulation techniques such as DCSK, CSK, COOK, and QCSK have a decision block at the output of the receiver circuit. The information signal at the output of this decision block is obtained by comparing it with the constant threshold voltage. When the modulation techniques used in noncoherent information transmission are examined, it can be seen that the most important disadvantage of these techniques is the use of the constant threshold voltage level, which could always change with the channel noise. When the adaptive threshold-COOK (AT-COOK) model that was proposed to overcome this problem in the literature is examined [15–17], it is observed that the noise signal at the receiver circuit is attempted to be obtained at the half period. In the structure given in Figure 2, the transmitter is composed a binary information module, an ultrawideband (UWB) chaotic generator and a modulator. The receiver is composed of two envelope detector (ED) modules, for estimating separately the chaotic radio pulse (CRP) energy and the noise energy, a subtractor. It is also expressed with bit duration T_b, bit energy E_b, noise energy N_0, and estimated noise energy N_0'. This is similar to the modulation known as chaotic masking in the literature. In the system of which the block scheme is given in Figure 2, the noise signal is obtained at the receiver circuit at the half period of the switching. The information signal is obtained by extracting this signal from the signal transmitted at the other half period. In the proposed method, the negative effect of the instantaneous noise variations is ignored. In addition, it was observed that the AT-COOK method gives better performance when compared to the proposed method in terms of performance. However, it has been observed in previous studies [16–18] that the AT-COOK method decreases the performance in environments where the ambient noise changes continuously, but gives a performance independent of noise in the proposed method. The most important advantage of the proposed method is that it is independent of noise. Furthermore, if the BER performance comparison is made with the AT-COOK [16] modulation technique, the proposed study performs better, especially at low and negative noise levels. This aspect stands out as an important advantage compared to all other models.

The design of a decision block that could be used in all of the DCC systems was aimed with the proposed ATL-COOK method. The decision block in the literature has two inputs. One of the inputs is constant threshold voltage level. In the novel receiver circuit, the decision block also has two inputs. One of them is the adaptive threshold voltage level. The information signal was simulated as a Dirac delta function in unit-impulse time. The purpose of simulating the information signal as a Dirac delta function is the use of this function's integral as the comparison curve for signal processing purposes [19]. In the novel proposed communication system, the signal that was squared at the input of the receiver circuit was used as the comparison signal at the decision block. The comparison signal that was used in the other input of the decision block was obtained by integrating the Dirac delta function. A second value was obtained for instantaneous comparison because the integral of the Dirac delta function is the ramp function. Theoretically, it seems possible to decrease the BER versus SNR to zero in the ideal operating conditions as shown in the mathematical expressions of the proposed system. When the simulation results are examined, it is shown that the dependency of the proposed method on the noise level was reduced. On the other hand, when these results are compared with the present DCC systems, it attracts attention with the same level BER ratios at various noise levels. Therefore, it is also advantageous that the model satisfies the system expectations with its predictable error rate in continuous operation.
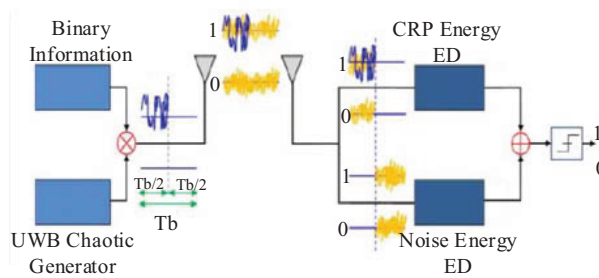

Figure 2. AT-COOK principle scheme [16].

As shown in Figure 3 the signal r(t) at the input of the novel receiver circuit is the same as that in the other DCC systems. Therefore, there is no difference with the other systems in terms of communication security. The fundamental improvement in the novel communication model is the reduction in the bit error rate at the recovery of the information signal. As shown in Figure 4 the decision mechanism of the receiver circuit in the proposed communication system can be expressed mathematically as follows:
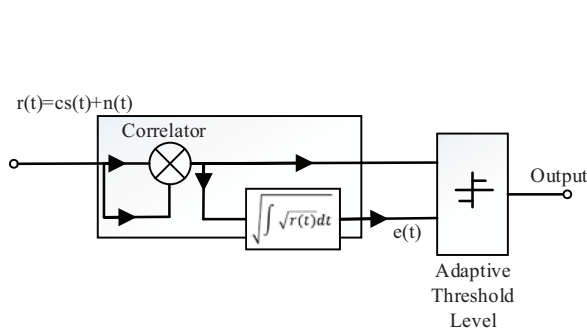

Figure 3. A new chaotic communication model: receiver circuit block.
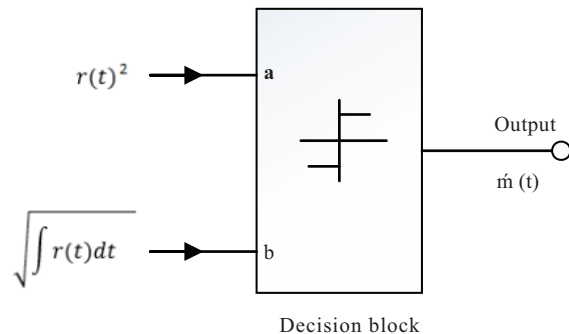

Figure 4. A new chaotic communication model receiver decision block.

In the ideal operating conditions (i.e. no noise)

$$r(t) = c.s(t) \tag{4}$$

Here s(t) is the transmitted signal at the switching moment of the transmitter circuit and c is the antenna gain of the transmitter circuit. For any time t, s(t) represents the direct delta function:

$$s(t) = \delta(t) \tag{5}$$

Thus, $r(t)^2 = (c.\delta(t))^2 = c^2.\delta(t)$. Therefore, the comparison signal when the switch equals "1" is

$$c^2.1 = c^2 \tag{6}$$

When the switch transmits a chaotic signal at the transmitter circuit, the input a of the decision block becomes c^2. When the switching signal is 0 at the transmitter circuit, the input a of the decision block becomes 0.

On the other hand, the signal at the other input of the decision block is

$$\sqrt{\int_{-\infty}^{t} c.\delta(t)dt} = \sqrt{c.u(t)} \tag{7}$$

Here $u(t)$ (Equation 8) is the unit step function (in other terms Heaviside theta function).

$$u(t-a) = \left\{ \begin{array}{ll} 0, & t < a \\ 1, & t > a \end{array} \right. , for \quad a = 0, \quad u(t) = \left\{ \begin{array}{ll} 0, & t < 0 \\ 1, & t > 0 \end{array} \right. \tag{8}$$

When the unit step function (i.e. u(t)) is integrated, the result is the ramp function (i.e. $ramp(t) = \int_{-\infty}^{t} u(t)dt$) expressed in Equation 9. The ramp function is used as the comparison signal in the second input of the decision block.

$$c.ramp(t) = c \int_{-\infty}^{t} u(t)dt = \left\{ \begin{array}{ll} 0, & t < 0 \\ c, & t \geq 0 \end{array} \right. \tag{9}$$

$$\widehat{m} = \left\{ \begin{array}{ll} 1, & a > b \\ 0, & a < b \end{array} \right. \tag{10}$$

The information signal m is obtained at the receiver circuit with the decision function expressed in Equation 10.

The red line in Figure 5 shows the ideal ramp function with no noise. The blue line shows the ramp function with the noise added in the simulation of the proposed communication system. Thus, the ramp function obtained from the comparison signal was used instead of the constant threshold voltage in the other digital communication systems. The results were obtained and interpreted using different chaotic generators for the proposed communication system.
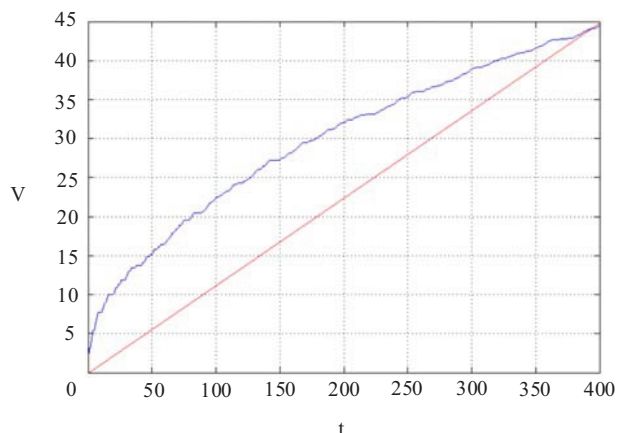
Figure 5. Ramp function curve (V-t); noiseless (red line) and noise added (blue line).

3. Simulations, results, and discussion

Simulation of the proposed ATL-COOK method and COOK communication system was conducted using different chaotic generators. The simulation was realized using Rössler, Sproot h, and Sproot n chaos signals with an AWGN noise between –6 dB and 15 dB. Simulation studies performed in agreement with the proposed method are demonstrated using different chaotic generators. In the study, while the fixed threshold value "0" is selected in the COOK communication system, the proposed system has created an adaptive threshold value. The simulation study was performed in Matlab Simulink. When the obtained results are examined, an increase of 90% in BER performance is observed with the proposed communication system. The results of the proposed study with the novel communication model are given below:

First, the Rössler chaotic generator given with dynamic Equation 7 was used. Rössler phase space and communication signals are shown in Figure 6 and Figure 7, respectively.
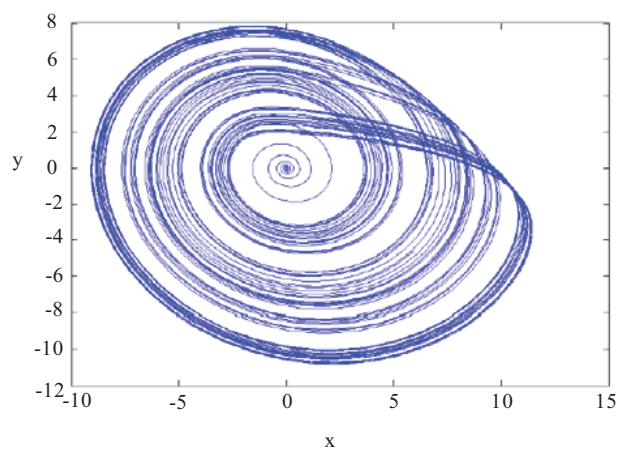

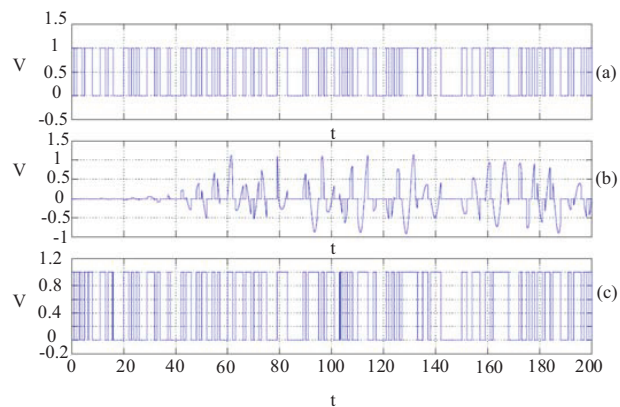**Figure 6**. Rössler chaotic attractor x, y plane.

Figure 7. Simulation results using the Rössler chaotic generator: (a) transmitted data signal, (b) signal at the receiving circuit input, (c) data signal obtained at the receiver.

$$\dot{x} = -y - z$$
$$\dot{y} = x + ay$$
$$\dot{z} = zx - zc + b \tag{11}$$

The analysis of the COOK communication system and the proposed ATL-COOK method was realized at various noise rates. Table 1 shows the number of errors and the error rate for different noise values. It can be seen that the BER versus SNR of the proposed model is very small. It can also be understood from Figure 8 that the BER versus SNR performances increased greatly. Similar work was done for the Sprott h chaotic generator. The dynamic system equations for the Sprott h chaotic generator are given by Equation 12.

Table 1. Communication system BER versus SNR rates with the Rössler chaotic generator.

Eb/No (db)	Rössler COOK communication system		Proposed new communication model with Rössler		Percentage decrease in proposed new communication model with Rössler
	Number of errors	Error rate	Number of errors	Error rate	% Percentage ratio
–6	736	0.18395401	65	0.01624594	91.17%
–5	627	0.15671082	53	0.01324669	91.55%
–4	536	0.13396651	44	0.01099725	91.79%
–3	455	0.11372157	32	0.00799800	92.97%
–2	387	0.09672582	27	0.00674831	93.02%
–1	311	0.07773057	24	0.00599850	92.28%
0	267	0.06673332	20	0.00499875	92.51%
1	244	0.06098475	18	0.00449888	92.62%
2	224	0.05598600	19	0.00474881	91.52%
3	216	0.05398650	16	0.00399900	92.59%
4	212	0.05298675	13	0.00324919	93.87%
5	211	0.05273682	13	0.00324919	93.84%
6	210	0.05248688	13	0.00324919	93.81%
7	210	0.05248688	12	0.00299925	94.29%
8	210	0.05248688	11	0.00274931	94.76%
9	210	0.05248688	10	0.00249938	95.24%
10	210	0.05248688	11	0.00274931	94.76%
11	210	0.05248688	11	0.00274931	94.76%
12	210	0.05248688	11	0.00274931	94.76%
13	210	0.05248688	11	0.00274931	94.76%
14	210	0.05248688	11	0.00274931	94.76%
15	210	0.05248688	11	0.00274931	94.76%
16	210	0.05248688	11	0.00274931	94.76%
17	210	0.05248688	11	0.00274931	94.76%
18	210	0.05248688	11	0.00274931	94.76%

The Sprott h chaotic generator given with dynamic Equation 7 was used. Sprott h phase space and communication signals are shown in Figures 9 and 10, respectively.

$$\dot{x} = -y + z^2$$
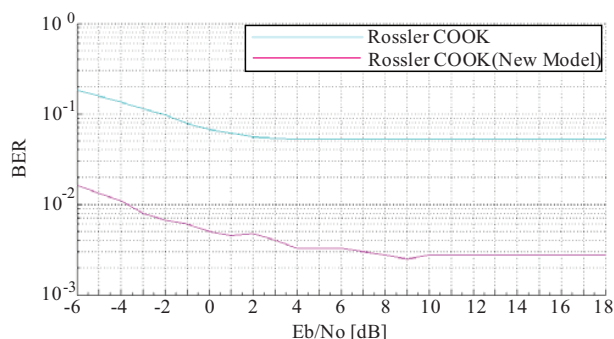$$\dot{y} = x + 0,5y$$
$$\dot{z} = x - z \tag{12}$$

Figure 8. BER versus SNR performance comparison studies using the Rössler chaos generator.
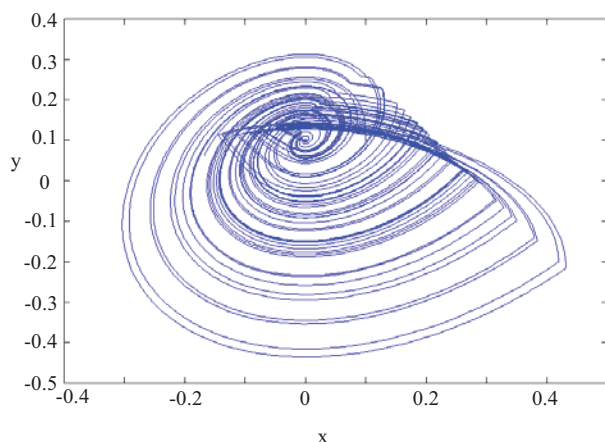
Figure 9. Sprott h chaotic attractor x, y phase space.
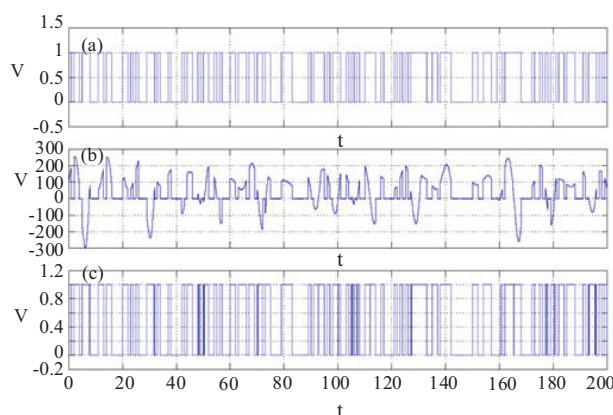

Figure 10. Simulation results using the Sprott h chaotic generator: (a) transmitted data signal, (b) signal at the receiving circuit input, (c) data signal obtained at the receiver.

Table 2 and Figure 11 show the results with the Sprott h chaos signal. It can be seen that the ATL-COOK method shows better performance. However, when the BER performance of Sprott h chaos generators is compared with that of other chaos generators, the switching times of the Sprott h chaos generators are long at some points (80, 140 time duration in Figure 10). The change in information signals at these locations increases the SNR rate. In other words, the Sprott h chaos generator has a different phase space representation, although other space chaos generators are single lobed. Finally, the analysis was repeated with the Sprott n chaos signal. Dynamic system equations are given by Equation 13. Furthermore, Sprott n phase space and communication signals are shown in Figures 12 and 13, respectively.

$$\dot{x} = -2y$$

$$\dot{y} = x + z^2$$

$$\dot{z} = 1 - y - 2z \qquad (13)$$

The results of the analysis with the Sprott n chaos signal are shown in Table 3 and Figure 14. The entire simulation results are shown in Figure 15. It can be seen that the error rates are high with the COOK model and the performance decreases when the noise level increases. BER versus SNR of the proposed ATL-COOK model is very small.

Table 2. Communication system BER versus SNR rates with the Sprott h chaotic generator.

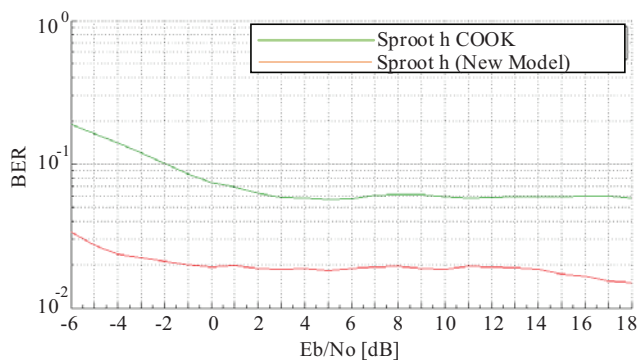| Eb/No (db)	Sprott h COOK communication system		Proposed new communication model with Sprott h		Percentage decrease in proposed new communication model with Sprott h
	Number of errors	Error rate	Number of errors	Error rate	% Percentage ratio
–6	756	0.188952762	135	0.033741565	82.14%
–5	651	0.162709323	110	0.027493127	83.10%
–4	560	0.139965009	94	0.023494126	83.21%
–3	480	0.119970007	89	0.022244439	81.46%
–2	406	0.101474631	84	0.020994751	79.31%
–1	342	0.08547863	80	0.019995001	76.61%
0	298	0.07448138	77	0.019245189	74.16%
1	277	0.069232692	79	0.019745064	71.48%
2	252	0.062984254	75	0.018745314	70.24%
3	235	0.058735316	74	0.018495376	68.51%
4	233	0.058235441	75	0.018745314	67.81%
5	226	0.056485879	73	0.018245439	67.70%
6	228	0.056985754	75	0.018745314	67.11%
7	242	0.060484879	77	0.019245189	68.18%
8	244	0.060984754	78	0.019495126	68.03%
9	245	0.061234691	75	0.018745314	69.39%
10	237	0.059235191	74	0.018495376	68.78%
11	233	0.058235441	78	0.019495126	66.52%
12	234	0.058485379	77	0.019245189	67.09%
13	238	0.059485129	76	0.018995251	68.07%
14	236	0.058985254	74	0.018495376	68.64%
15	236	0.058985254	69	0.017245689	70.76%
16	239	0.059735066	66	0.016495876	72.38%
17	241	0.060234941	61	0.015246188	74.69%
18	231	0.057735566	60	0.014996251	74.03%

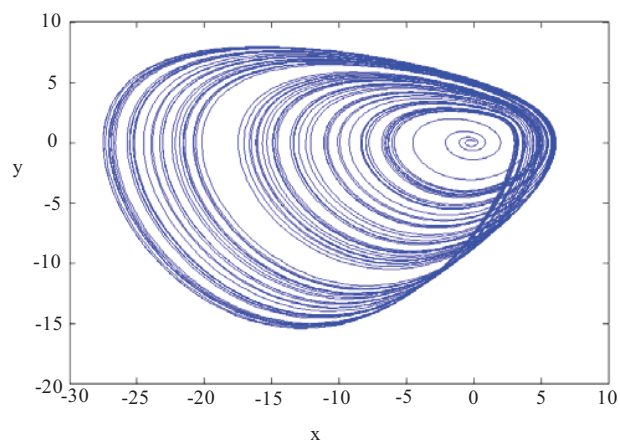**Figure 11**. BER versus SNR performance comparison using the Sprott h chaos generator.

Figure 12. Sprott n chaotic attractor x, y phase space.

Table 3. Communication system BER versus SNR rates with the Sprott n chaotic generator.

| Eb/No (db)	Sprott n COOK communication system		Proposed new communication model with Sprott n		Percentage decrease in proposed new communication model with Sprott n
	Number of errors	Error rate	Number of errors	Error rate	% Percentage ratio
−6	728	0.181954511	33	0.008247938	95.47%
−5	619	0.154711322	28	0.00699825	95.48%
−4	527	0.131717071	25	0.006248438	95.26%
−3	449	0.112221945	20	0.00499875	95.55%
−2	378	0.094476381	14	0.003499125	96.30%
−1	303	0.075731067	15	0.003749063	95.05%
0	260	0.064983754	13	0.003249188	95.00%
1	238	0.059485129	12	0.00299925	94.96%
2	216	0.053986503	12	0.00299925	94.44%
3	208	0.051987003	10	0.002499375	95.19%
4	205	0.051237191	11	0.002749313	94.63%
5	205	0.051237191	8	0.0019995	96.10%
6	203	0.050737316	7	0.001749563	96.55%
7	203	0.050737316	6	0.001499625	97.04%
8	204	0.050987253	6	0.001499625	97.06%
9	204	0.050987253	5	0.001249688	97.55%
10	204	0.050987253	6	0.001499625	97.06%
11	204	0.050987253	9	0.002249438	95.59%
12	205	0.051237191	7	0.001749563	96.59%
13	204	0.050987253	6	0.001499625	97.06%
14	204	0.050987253	7	0.001749563	96.57%
15	204	0.050987253	7	0.001749563	96.57%
16	204	0.050987253	7	0.001749563	96.57%
17	205	0.051237191	8	0.0019995	96.10%
18	204	0.050987253	6	0.001499625	97.06%
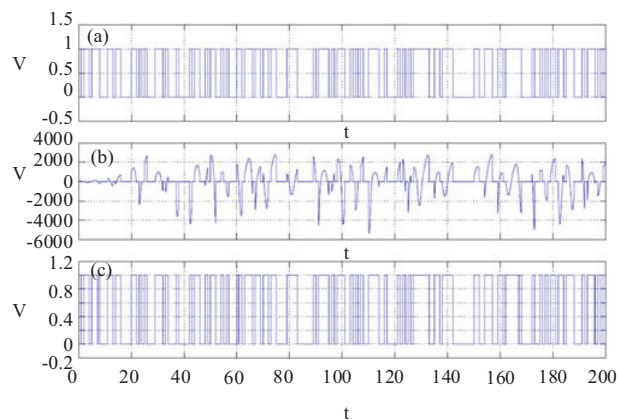
Figure 13. Simulation results using the Sprott n chaotic generator: (a) transmitted data signal, (b) signal at the receiving circuit input, (c) data signal obtained at the receiver.
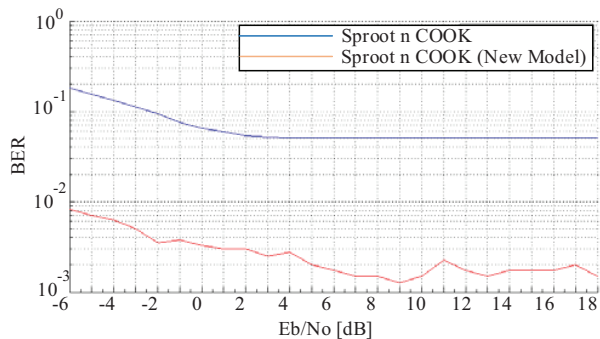

Figure 14. BER versus SNR performance comparison studies using the Sprott n chaos generator.
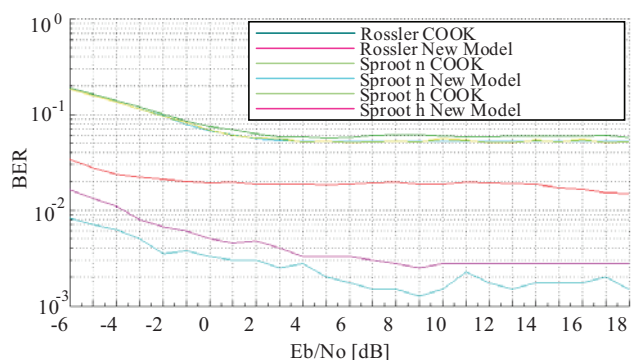
Figure 15. BER versus SNR performance comparison studies using different continuous chaos generators in the COOK communication system and the proposed communication system in Matlab Simulink.

4. Experimental realization of the proposed ATL-COOK on FPAA

The same simulation scenarios were repeated experimentally using field programmable analogue arrays (FPAAs). The chaos signal becomes periodic after a moment in the experiments done with digital hardware. The reliability of the communication system decreases when the chaos signal is periodic. Therefore, the use of noncoherent structures became much more important in analogue-based chaotic communication systems [20].

The ability to implement the ATL-COOK method in FPAA platforms is another advantage of the method. Four FPAA blocks were used in the experimental study. The Rössler chaos signal was obtained in the FPAA1 block. The resulting chaos signal was transferred to the FPAA2 block. The FPAA2 block uses PERIODIC WAVE BLOCK, where the information signal and ambient noise are modeled. In addition, in the FPAA2 block, the GAINSWITCH block was used to switch the signal to the transmitted signal by adding ambient noise to the transmitted signal. The signal switched on the AWGN signal and the GAINSWITCH block was transferred to the FPAA3 block. These two signals from the FPAA2 block were collected using the SUMINVERTER BLOCK and a transmission medium signal was obtained. In addition, in the FPAA3 block, the correlator operation at the receiver circuit was performed using the TRANSFER FUNCTION and transferred to the FPAA4 block. In the FPAA4 block, the first signal at the comparator input was obtained from the signal INTEGRATOR in the correlator output signal. The second signal at the comparator input was obtained using the TRANSFER FUNCTION. The signal at the comparator output was transferred from the FPAA4 block to the output. The FPAA realization scheme of the ATL-COOK communication system is shown in Figure 16. Table 4 presents the blocks and their purposes used in the FPAA realization scheme.
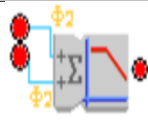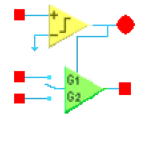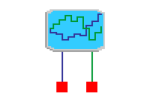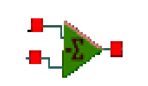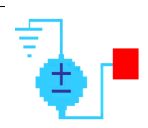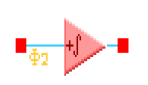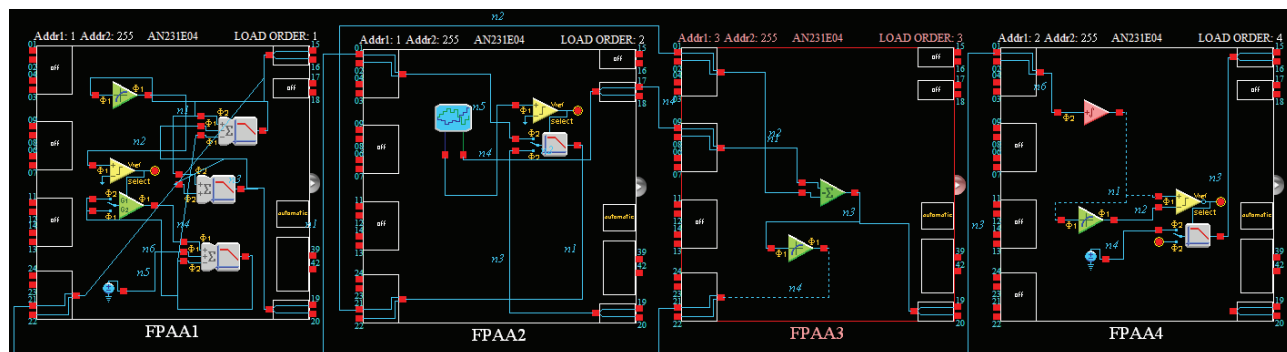

Figure 16. FPAA implementation of the proposed receiver circuit: (a) Rössler chaotic generator is presented in FPAA1, (b) transmitting circuit and noise signal generator in FPAA2, (c) addition of AWGN with modulation signal in FPAA3, (d) realization of the proposed system in FPAA4.

The software was deployed in the FPAA development card after it was modeled in the interface. The input and output information signals were measured experimentally using a digital oscilloscope via input/output terminals of the FPAA development card.

The experimental implementation was performed with the Rössler chaos signal on FPAA1. Dynamic system equations and phase space of the Rössler chaos signal are given by Equation 11 and Figure 17, respectively. The information signal to be transmitted is shown in Figure 18. The information signal is used for switching of the chaotic generator in the communication system. Switching with the information signal was realized with the GAINSWITCH block in the experimental study.

Figure 19 shows the communication signal with added noise in the receiver circuit input. This received signal was used in obtaining the decision block signals by correlating it in the receiver circuit.

Table 4. FPAA realization blocks used in the experimental study.

FPAA Realization Blocks		
SUMFILTER BLOCK		SUMFILTER blocks work as an integrator by using Laplace transforms, and are used to obtain state equations of the chaotic generator in FPAA1. SumFilter1; Gain1=1, Gain2=1, Gain3=1, Corner Frequency=1.2 kHz. SumFilter2; Gain1=1,Gain2=1.25, Corner Frequency=1.2 kHz. SumFilter3; Gain1=1, Gain2=0.6, Gain3=2, Corner Frequency=1.2 kHz.
TRANSFER FUNCTION		TRANSFER FUNCTION in FPAA1 is used for implementation of PWL-based output function of the system. On the other hand, *TRANSFER FUNCTION* in FPAA3 and in FPAA4 performs the math function in the correlator block.
GAINSWITCH BLOCK		GAINSWITCH block is used to obtain switching and thresholding processes. *GAINSWITCH* block in FPAA1 is used in the Rössler chaotic generator.
PERIODIC WAVE BLOCK		PERIODIC WAVE block is used in FPAA2 for generating the data signal, which is a Bernoulli binary generator, in transmitter block, and also used for additive white Gaussian noise in FPAA3.
SUMINVERTER BLOCK		SUMINVERTER block is used for adding AWGN and modulation signal in FPAA3.
DC VOLTAGE SOURCE BLOCK		DC VOLTAGE SOURCE block provides constant values of Rössler chaotic generator in FPAA1.
INTEGRATOR		INTEGRATOR block works as an integrator in FPAA4.

The information signal obtained at the output of the decision block is shown in Figure 20. The results of the experimental study were obtained from the digital oscilloscope. The experimental results are shown in Figure 21.

Figure 21 shows the BER versus SNR comparison for COOK and ATL-COOK. It can clearly be seen that the BER versus SNR of the proposed model has better performance. The experimental results are similar to the simulation results.
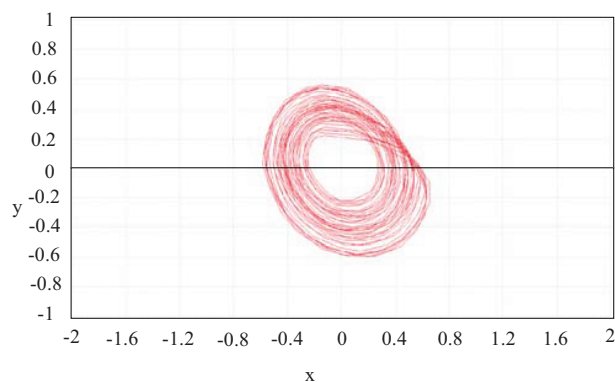

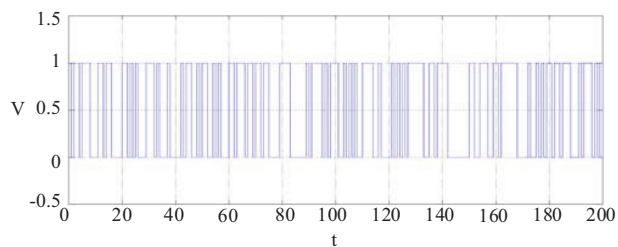**Figure 17**. Rossler chaotic attractor x, y phase space.
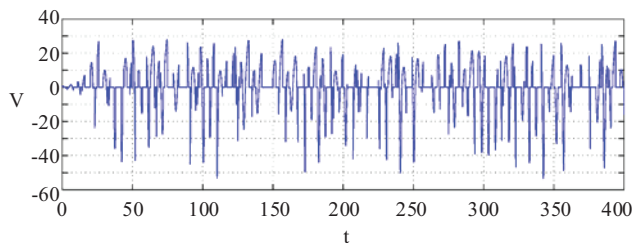

Figure 18. Transmitted data signal.

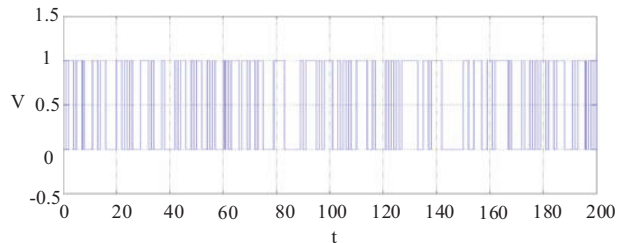**Figure 19**. Signal at the receiving circuit input.

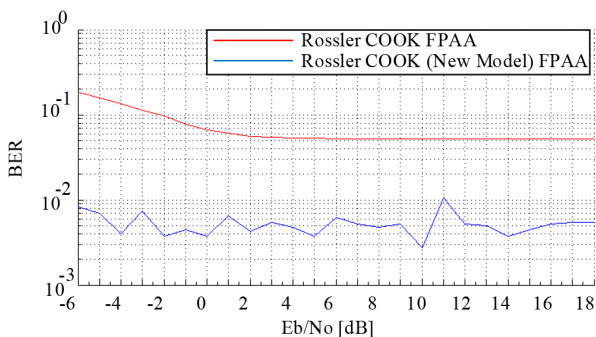**Figure 20**. Data signal obtained at the receiver.

Figure 21. BER versus SNR performance comparison studies using the Rössler chaos generator in the COOK communication system and the proposed communication system in the FPAA platform.

5. Conclusion

A novel decision block was proposed for distributed spectrum DCC systems with the present study. A decision block with an adaptive threshold voltage level was realized for noncoherent structures with the proposed method. The proposed method was called ATL-COOK because the threshold voltage level can change instantaneously. The simulation of the proposed method was done using different chaos signals and it was verified that it has a better error performance than the COOK system. As a result of the simulation and experimental studies, it is observed that the proposed method increases the application areas of DCC systems in wireless communication systems as it obviates the noise effect on chaotic communication systems. Furthermore, the method is also important not just with its bit error rate but also its applicability to reconfigurable analogue systems. In future work we will consider improving the bit error rate of DCC systems to be acceptable for reliable communication systems.

References

[1] Lorenz EN. Deterministic nonperiodic flow. Journal of the Atmospheric Sciences 1963; 20: 130-141.

[2] Kennedy MP, Kolumban G, Jako Z. Chaotic modulation schemes. In: Kennedy M, Rovatti R, Setti G (editors). Chaotic Electronics in Telecommunications. 1st ed. Boca Raton, FL, USA: CRC Press, 2000, pp. 151-183.

[3] Cuomo KM, Oppenheim AV, Strogatz SH. Synchronization of Lorenz-based chaotic circuits with applications to communications. IEEE Transactions on Circuits and Systems-II: Analog and Digital Signal Processing 1993; 40: 626-633.

[4] Kennedy MP, Kolumbán G. Digital communications using chaos. Signal Processing 2000; 80 (7): 1307-1320.

[5] Chua LO, Desoer CA, Kuh ES. Linear and Nonlinear Circuits. New York, NY, USA: McGraw-Hill, 1987.

[6] Dedieu H, Kennedy M, Hasler M. Chaos shift keying: modulation and demodulation of a chaotic carrier using self-synchronizing Chua's circuits. IEEE Transactions on Circuits and Systems II 1993; 40 (10): 634-643.

[7] Abdullah H, Valenzuela A. Performance evaluation of FM-COOK chaotic communication system. Journal of Signal and Information Processing 2011; 2 (3): 175-177.

[8] Kolumban G, Kennedy MP, Kis G. Performance improvement of chaotic communications systems. In: 1997 European Conference on Circuit Theory and Design (ECCTD); Budapest, Hungary; 1997. pp. 284-289.

[9] Kolumbàn G, Vizvari G, Schwarz W. Differential chaos shift keying: a robust coding for chaos communication. In: 1996 Proceedings of International Workshop on Nonlinear Dynamics of Electronic Systems (NDES); Seville, Spain; 1996. 1 (1): 87-92.

[10] Chua L, Yang L. Cellular neural networks: theory. IEEE Transactions on Circuits and Systems 1988; 35 (10): 732–745.

[11] Chua LO, Yang L. Cellular neural networks: applications. IEEE Transactions on Circuits and Systems 1988; 35 (10): 1273-1290.

[12] Pecora LM, Carroll TL. Synchronization in chaotic systems. Physical Review Letters 1990; 64: 821-824.

[13] Carroll TL, Pecaro LM. Synchronizing chaotic circuits. IEEE Transactions on Circuits and Systems 1991; 38 (4): 453-456.

[14] Pecora LM, Carroll TL. Driving systems with chaotic signals. Physical Review A 1991; 44: 2374-2383.

[15] Dmitriev AS, Hasler M, Panas AI, Zakharchenko KV. Basic principles of direct chaotic communications. In: Pikovsky A, Maistrenko Y (editors). Synchronization: Theory and Application. Dordrecht, Netherlands: Springer, 2003, pp. 41-63.

[16] Said S, Tanougast C, Salah AM. Novel adaptive decision threshold modulation technique for UWB direct chaotic communications. Journal of Engineering Science Technology Review 2015; 8 (2): 1-7.

[17] Mesloub A, Boukhelifa A, Merad O, Saddoudi S, Younsi A et al. Chip averaging chaotic ON–OFF keying: a new non-coherent modulation for ultra wide band direct chaotic communication. IEEE Communications Letters 2017; 21 (10): 2166-2169.

[18] Maali A, Mesloub A, Djeddou M, Mimoun H, Baudoin G et al. Adaptive CA-CFAR threshold for non-coherent IR-UWB energy detector receivers. IEEE Communications Letters 2009; 13 (12): 959-961.

[19] Adebola E, Olabiyi O, Annamalai A. On the Dirac delta approximation and the MGF method for ASER analyses of digital communications over fading channels. IEEE Communications Letters 2013; 17 (2): 245-248.

[20] Günay E, Altun K. BER analysis and application in FPGA and FPAA based communication systems. In: 2017 International Artificial Intelligence and Data Processing Symposium (IDAP); Malatya, Turkey; 2017. pp. 1-5.